Coordinated multiplexing of information about separate objects in visual cortex

Na Young Jun (1-3)
Douglas A. Ruff (4-5)
Lily E. Kramer (4-5)
Brittany Bowes (4-5)
Surya T Tokdar (6)
Marlene R Cohen (4-5)
Jennifer M Groh (1-3, 7-9)

1. Department of Neurobiology, Duke University
2. Center for Cognitive Neuroscience, Duke University
3. Duke Institute for Brain Sciences
4. Department of Neuroscience, University of Pittsburgh
5. Center for the Neural Basis of Cognition, University of Pittsburgh
6. Department of Statistical Science, Duke University
7. Department of Psychology and Neuroscience, Duke University
8. Department of Biomedical Engineering, Duke University
9. Department of Computer Science, Duke University

Acknowledgments:

Thanks to: Valeria C. Caruso, Yunran Chen, Jeffrey T. Mohl, Meredith N. Schmehl, Shawn M. Willett, for helpful comments on the analysis and manuscript. This work was supported by: National Institutes of Health grant nos. R00EY020844 (MRC), R01EY022930 (MRC); Core Grant P30 EY008098s (MRC); R01DC013906 (JMG, STT); and R01DC016363 (JMG, STT); and by support to MRC from the McKnight, Whitehall, Sloan and Simons Foundations.

Abstract

Sensory receptive fields are large enough that they can contain more than one perceptible stimulus. How, then, can the brain encode information about *each* of the stimuli that may be present at a given moment? We recently showed that when more than one stimulus is present, single neurons can fluctuate between coding one vs. the other(s) across some time period, suggesting a form of neural multiplexing of different stimuli (Caruso et al., 2018). Here we investigate (a) whether such coding fluctuations occur in early visual cortical areas; (b) how coding fluctuations are coordinated across the neural population; and (c) how coordinated coding fluctuations depend on the parsing of stimuli into separate vs. fused objects. We found coding fluctuations do occur in V1 but only when the two stimuli form separate objects. Such separate objects evoked a novel pattern of V1 spike count ("noise") correlations involving distinct distributions of positive and negative values. This bimodal correlation pattern was most pronounced among pairs of neurons showing the strongest evidence for coding fluctuations or multiplexing. Whether a given pair of neurons exhibited positive or negative correlations

depended on whether the two neurons both responded better to the same object or had different object preferences. Distinct distributions of spike count correlations based on stimulus preferences were also seen in V4 for separate objects but not when two stimuli fused to form one object. These findings suggest multiple objects evoke different response dynamics than those evoked by single stimuli, lending support to the multiplexing hypothesis and suggesting a means by which information about multiple objects can be preserved despite the apparent coarseness of sensory coding.

Significance Statement

How the brain separates information about multiple objects despite overlap in the neurons responsive to each item is not well understood. Here we show that some neurons in V1 exhibit coding fluctuations in response to two objects, and that these coding fluctuations are coordinated at the population level in ways that are not observed for single objects. Broadly similar results were obtained in V4. These response dynamics lend support to the hypothesis that information about individual objects may be multiplexed across the neural population, preserving information about each item despite the coarseness of sensory coding.

Key Words

Spike count correlations; variability; V1; multiplexing; attention; population coding

Introduction

Coarse population coding has been widely explored in motor systems, where neurons show broad activity profiles and are thought to “vote” for the movement typically associated with their peak activity (e.g. (Georgopoulos et al., 1986; Lee et al., 1988)). However, individual motor systems only generate one movement at a time. Such a coarse coding/population voting scheme cannot work in sensory systems where there are generally many stimuli to be represented rather than a single (e.g. arm or eye) movement to be specified. It has been assumed that sensory receptive fields are small enough that coarse coding does not apply, but this seems questionable. For example, the letters on the page you are reading now are probably < 0.25 degree apart, but foveal V1 receptive fields are approximately 0.5-2 degrees in diameter (Dow et al., 1981; Alonso and Chen, 2009; Keliris et al., 2019). Receptive fields get even larger at later stages along the visual processing stream (e.g. Alonso and Chen, 2009). In the auditory system, mammalian neurons may be responsive to nearly any location in space (e.g. Woods et al., 2001; Groh et al., 2003; McAlpine and Grothe, 2003; Werner-Reiss and Groh, 2008; Grothe et al., 2010; Higgins et al., 2010) and even frequency tuning is broad at conversational sound levels (Bulkin and Groh, 2011; Willett and Groh, 2022). Such breadth of tuning means that there can be overlap in the population of neurons activated by individual stimuli, making it unclear how information about multiple objects is preserved.

Logic suggests that information about each distinct stimulus must be segregated within the neural code in some fashion, either into exclusive neural subpopulations, different epochs of time, or some combination of both. We have recently presented the hypothesis that the nervous system might employ a form of neural turn-taking, (time division multiplexing) in which individual neurons fluctuate between responding to each of the items in or near their receptive fields across various epochs of time (Caruso et al., 2018; Mohl et al., 2020). Such a coding scheme could preserve information about each stimulus across time and/or across neural subpopulations.

This theory raises three key open questions. First, is multiplexing a general phenomenon that occurs across a range of different brain areas? Our original study tested one subcortical auditory area (the inferior colliculus) and one extrastriate visual cortical area (area MF of the inferotemporal (IT) face patch system). More areas need to be tested to understand how such a coding scheme might operate. Second, in brain areas that exhibit such coding fluctuations, do neurons fluctuate together and if so, how? Pairs of neurons might show positive, negative, or no correlations with each other. The pattern of such correlations across the population can reveal whether the population as a whole retains information about both stimuli and whether there is bias favoring one stimulus over another.

Third, does the pattern of fluctuations depend on the parsing of the scene into separate objects? Individual stimuli can fuse into one object or be perceived as distinct from each other. Stimuli that segregate into separate objects may be more likely to be associated with fluctuations in neural activity and their attendant correlations across neurons (Milner, 1974; Gray and Singer, 1989; Von Der Malsburg, 1994; Singer and Gray, 1995; Gray, 1999) (but see Palanca and DeAngelis, 2005), whereas stimuli that fuse into a single distinct object may cause activity patterns that are akin to those observed when only one stimulus is present. Such a pattern would specifically implicate activity fluctuations in playing a role in the perceptual process of object segregation.

To address these questions, we turned to the primary visual cortex (V1). V1 allows for a strong test of these hypotheses since V1 neurons have comparatively small receptive fields and are therefore less subject to the multiple-stimulus-overlap problem than the more broadly tuned areas such as the inferior colliculus or inferotemporal (IT) cortex that were assessed in our previous report (Caruso et al., 2018). Even though V1 neurons themselves have comparatively small receptive fields, V1 contributes to processing in higher cortical areas where spatial tuning is coarser. V1 could therefore also exhibit fluctuating activity patterns so as to facilitate preservation of information about multiple stimuli at higher stages.

We evaluated activity in V1 while monkeys viewed either individual stimuli (gratings) or two different types of combined stimuli (superimposed vs. adjacent gratings). When the two gratings were superimposed, they presumably appeared as one fused object, or plaid (Adelson and Movshon, 1982; Rodman and Albright, 1989; Heeger et al., 1996; Busse et al., 2009; Lima et al., 2010), whereas when they were adjacent they appeared as

two distinct objects. We found evidence for coding fluctuations when two gratings were present at separate locations (two objects) but not when the gratings were superimposed at the same location and appeared as one fused object. We then evaluated the degree and sign of the spike count correlations (commonly referred to as "noise" correlations (Cohen and Kohn, 2011)) observed between pairs of simultaneously recorded units in response to presentations of particular stimulus conditions. We found that the pattern of correlations varied dramatically depending on whether the stimuli were presented either individually or superimposed (single stimuli or one fused object) vs. when they were presented side-by-side (two separate objects). In the two-object case, the distribution of spike count correlations was markedly different from previous reports involving individual stimuli (c.f. Table 1, Cohen and Kohn, 2011) , and encompassed a range spanning many negative correlations in addition to positive ones. Whether the correlations tended to be positive vs. negative depended on whether the two neurons in the pair preferred the same stimulus (median correlation +0.25) or preferred different stimuli (median correlation -0.05). The distribution of spike count correlation values was even more widely spread among pairs of neurons that showed demonstrably fluctuating activity across stimulus presentations (same preference: +0.49 and different preference: -0.14). In contrast, in the single stimuli and fused object (superimposed gratings) cases, positive correlations predominated (single stimuli: median value 0.15-0.19; fused object: median value +0.15). Distinct tuning-preference-related distributions of spike count correlations for adjacent stimuli but not for superimposed/fused stimuli were also seen in a smaller additional dataset in V4.

Overall, this pattern of results is consistent with the possibility that when two visual objects are presented in close proximity, a subpopulation of visual cortical neurons fluctuates in a coordinated fashion, generally retaining information about segregated objects and suggesting an account for why they can be perceived at once.

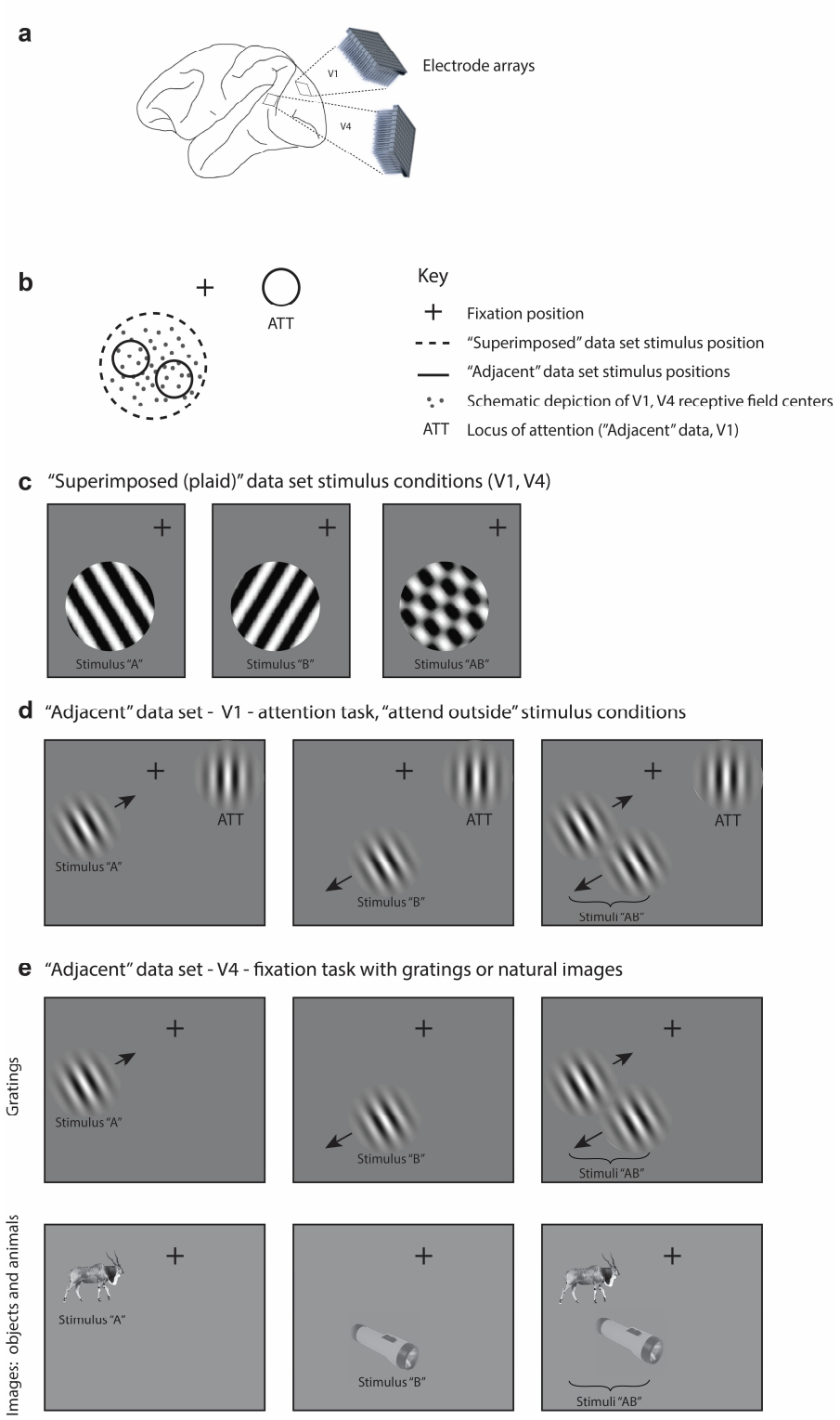

Figure 1. Experimental design. A. Multiunit activity was recorded in V1 and V4 using chronically implanted 10x10 or 6x8 electrode arrays in six monkeys (see Methods). B. In both "superimposed" and "adjacent" datasets, the stimuli were positioned to overlap with ("adjacent" dataset) or completely span ("superimposed" dataset) the centers of the receptive fields of the recorded neurons. C. In the "superimposed" dataset, gratings were presented either individually or in combination at a consistent location and were large enough to cover the V1 and V4 receptive fields (stimulus size range: 2.5-7°). The combined gratings appeared as a plaid (rightmost

panel). Monkeys maintained fixation throughout stimulus presentation and performed no other task. D. In the V1 "adjacent" dataset, Gabor patches were smaller (typically ~1°) and were presented individually or side-by-side roughly covering the region of the V1 receptive fields. Monkeys maintained fixation while performing an orientation change detection task. The data analyzed in this study involved trials in which the monkeys were attending a third Gabor patch located in the ipsilateral hemifield to perform the orientation change detection. E. In the V4 "adjacent" dataset, the stimuli consisted of either Gabor patches or natural image stimuli, and monkeys performed a fixation task. Incorrectly performed trials and stimulus presentations during which we detected microsaccades are excluded from all analyses.

Results

General experimental design

The activity of neurons in visual cortex was recorded in three experimental designs in six monkeys (N=2 per experiment per brain area), using chronically implanted multielectrode arrays (Fig 1a, Table 1 in Methods). In the "superimposed" data set, the activity of neurons in V1 and V4 was recorded while monkeys passively fixated (for details, see (Ruff et al., 2016). In the "adjacent" data sets, the activity of V1 and V4 neurons were recorded while monkeys either passively fixated (V4 recordings) or fixated while performing an orientation change discrimination task involving either one of these stimuli or a third stimulus presented in the ipsilateral hemifield (V1) (for details, see (Ruff and Cohen, 2016). In the "superimposed" data set, the gratings were large, spanning the receptive fields of the recorded neurons, and were presented either individually or in combinations of two orthogonal gratings at a consistent location on every trial (Fig 1c). When the two gratings were presented, they superimposed and formed one fused "plaid" object. In the "adjacent" data sets, the stimuli were smaller Gabor patches (V1, V4, Figure 1d-e) or natural images (V4, Figure 1e, stimuli from (Long et al., 2018)) and were presented either individually or adjacent to one another as two separate objects. Together they spanned the receptive fields of the V1 or V4 neurons being recorded in a fashion similar to the "superimposed" experiment. For data collected during performance of the attention task (V1), we focused our analyses on trials in which the monkeys attended to the third stimulus and judged its orientation, i.e. attention was consistently directed away from either of the two adjacent Gabor patches that elicited responses in the neurons under study (Figure 1d). Trials in which the monkey was required to attend to one or the other of the adjacent Gabor patches were excluded from the analyses, as were incorrectly performed trials.

Any potential contribution of eye movements and/or fixation variation to visually-evoked activity was minimized as follows: 1) Fixation windows were small, +/- 0.5 degrees horizontally and vertically, and trials with broken fixations were excluded from further analysis. 2) Any trials with microsaccades during the stimulus presentations (defined as eye velocity exceeding 6 standard deviations above the mean velocity observed during steady fixation, (Engbert and Kliegl, 2003)) were excluded from further analysis. 3) Only a 200 ms period after stimulus onset was analyzed. Our reasoning is that any stimulus-evoked modulation in eye position would have a latency of 150-350 ms (Engbert and Kliegl, 2003)). This would have limited the consequences of any

potential stimulus-evoked fixational modulation to at most only roughly the last 50 ms of the 200 ms spike counting window. In addition, we verified that there actually was no difference in eye position variation based on the stimulus conditions (Supplementary Figure 2), so even this slim possibility was not borne out.

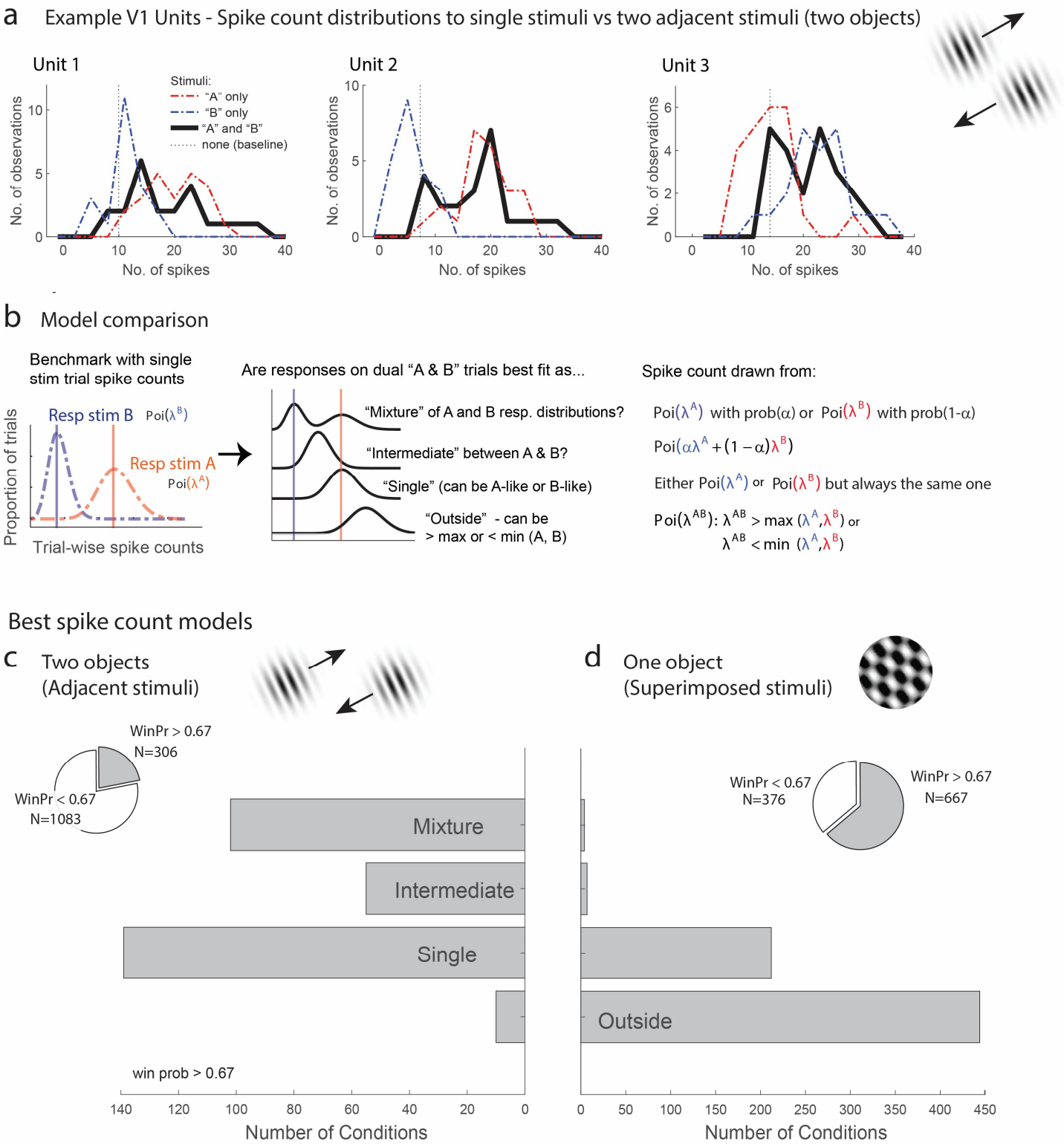

Figure 2. Examples of V1 units showing fluctuating activity pattern and formal statistical analysis. A. Distribution of spike counts on single stimuli (red, blue) and dual adjacent stimulus presentations (black) for three units in V1 tested with adjacent stimuli. Spikes were counted in a 200 ms window following stimulus onset. B. Bayesian model comparison regarding spike count distributions. We evaluated the distribution of spike counts on combined stimulus presentations in relation to the distributions observed on when individual stimuli were presented alone. Four possible models were considered as described in the equations and text. Only one case each of the "single" (B-like) and "outside" ($\lambda^{AB} > \max(\lambda^{A}, \lambda^{B})$ is shown. C, D. Best spike count models for the adjacent (C) and superimposed (D) stimulus datasets, meeting a minimum winning probability of at least 0.67, i.e. the winning model is at least twice as likely as the best alternative. Pie chart insets illustrate proportion of tested conditions that met this confidence threshold. While "singles" dominated in the adjacent stimulus dataset and "singles" and "outsides" dominated in the superimposed stimulus datasets, we focus on the presence of a "mixtures" as an important minority subpopulation present nearly exclusively in the "adjacent" stimulus dataset.

Two objects evoke fluctuating activity patterns in V1

We first evaluated the response patterns for evidence of fluctuating activity profiles consistent with multiplexing of information on multistimulus trials. Figure 2A illustrates three V1 example units from the adjacent-stimuli dataset, each of which showed spike count distributions on dual stimulus presentations (black lines, 200 ms spike-counting window) that reflected a mixture of the distributions evident on the corresponding single stimulus presentations (red and blue lines). The dual-stimulus distributions of spike counts are over-dispersed compared to what would be expected if the spikes on dual stimulus presentations were generated from a similar Poisson process as the single stimulus presentations, and a tendency for bimodality with modes near the modes for each of the individual stimulus presentations is evident.

While it is visually evident that the spiking responses of these three V1 example units on combined AB stimulus presentations appear drawn from a mixture of the A-like and B-like response distributions, evaluating this systematically across the population requires a formal statistical assessment. We developed such an assessment in our previous work concerning fluctuating activity in the context of encoding of multiple simultaneous stimuli (Caruso et al., 2018; Mohl et al., 2020; Glynn et al., 2021). In particular, we can model the firing rate behavior of neurons when two simultaneous grating stimuli A and B are presented in relation to the firing rates that occur when stimuli A and B are presented individually. We assume that each single-stimulus condition induces Poisson-distributed spike counts and we exclude cases where this assumption is violated (see Methods for details). We use a Bayesian model comparison framework to consider four hypotheses concerning the combined AB stimulus presentations (Figure 2B): 1) The responses to A and B together appear drawn from the same distribution as either A or B and consistently so on every stimulus presentation, as if the unit responded to only one of the two stimuli ('*single'*). 2) Responses to A and B together appear drawn from a distribution '*outside'* the range spanned by the A and B response distributions; this is the predicted pattern if neurons generally exhibited enhanced responses to combined AB stimuli than either stimulus alone, or if one stimulus strongly suppressed the response to the other. 3) The responses to A and B together are drawn from a single

distribution with a mean at an '*intermediate'* value between the A-like and B-like response rates. This is the response pattern that would be expected under theories such as divisive normalization in which the responses of an individual neuron to a more favored stimulus are reduced when other stimuli are also present, but can also represent fluctuating activity on a fast, sub-stimulus-duration timescale, as shown for some neurons in the IT face patch system and inferior colliculus (Caruso et al., 2018). 4) The responses to A and B together appear to be drawn from a '*mixture'* of the A-like and B-like response distributions. Mixtures are the category of interest for this analysis, as they indicate the presence of activity fluctuations at the stimulus-presentation timescale.

The overall presence of "mixtures" in V1 differed substantially depending on whether one object or two was presented (the superimposed vs. adjacent grating datasets). Figure 2C shows the results for conditions that produced a winning model that was at least twice as likely as its nearest competitor ("win prob > 0.67", the full results are provided in Supplementary Figure 3). We found that "mixtures" were evident in a third of V1 units (33%) when two objects were presented (adjacent gratings, Figure 2C), but were very rare when only one "object" was present (superimposed gratings, Figure 2D, 2%). The incidence of "mixtures" in V1 for the adjacent stimuli was slightly below that observed in the MF face patch in IT cortex (38%) and about half the rate observed in the inferior colliculus (67%; IT and IC data re-analyzed from Caruso et al. 2018 to use similar winning model criteria as shown here for the present study). The remainder of the tested conditions were best explained by the 'single' hypotheses for the adjacent stimuli, indicating winner (or loser) -take-all response patterns, or a blend of 'single' and 'outside' for the superimposed plaid stimuli, indicating the predominance of winner/loser-take-all and either enhancement or suppression in this dataset (see also Supplementary Figure 3). This "single" vs. "single-or-outside" difference almost certainly stems from differences in the size of the stimuli being presented in these two datasets -- typically only one of the two adjacent gratings was located within the classical receptive field of a given V1 unit whereas this was often not the case for the superimposed dataset. This difference is a side note to our main focus on the fluctuating activity patterns that do occur in V1 in response to multiple objects but not in response to individual objects.

Possible ways fluctuating activity might be coordinated across the population

Our next question concerns how fluctuating activity patterns are coordinated at the population level, and the implications for preserving information about each of the stimuli that are present. To assess such coordination, we computed Pearson's correlation between the spike count responses observed during presentations a given stimulus combination for pairs of units in each data set (spike count correlation, r_{sc}, also commonly called a noise correlation). We begin by discussing the possible results and their interpretation schematically in Figures 3 and 4. The overall point is that the activity of pairs of neurons might be either positively or negatively correlated, and the interpretation of such correlation patterns will depend on the turning preferences of the two neurons in the pair.

Figure 3 illustrates potential correlation patterns for pairs of several hypothetical neurons, each having a “mixture” response patterns, but two with a similar or “congruent” individual stimulus preference (Unit 1, Unit 2, more spikes elicited by “A” than “B” when presented alone) and one with a different stimulus preference compared to the other two (Unit 3, more spikes elicited by “B” than “A” when presented alone, “incongruent”) (Figure 3A). When spike count correlations are computed across trials in which both “A” and “B” are presented, four different scenarios (or combinations thereof) could occur. “Congruent” Units 1 and 2 could be positively correlated, suggesting they are encoding the same stimulus on the same trials (i.e. both “A” or both “B”, Figure 3B, left). Alternatively, they could be negatively correlated, suggesting they are encoding different stimuli on different trials (i.e. one “A” and the other “B”, Figure 3C,left). Conversely, when considering the spike count correlations between pairs of neurons exhibiting “incongruent” stimulus preferences (e.g. a “B” preferring Unit 3 vs. the “A” preferring Unit 1), the opposite applies – a positive correlation would be consistent with the two neurons encoding different stimuli in concert (Figure 3C, right), and a negative correlation would be consistent with encoding the same stimulus in concert (Figure 3C, left). In short, positive vs. negative spike count correlations in response to combined stimuli will have different interpretations depending on whether the two neurons in the pair both respond more vigorously to the same component stimulus or to different component stimuli.

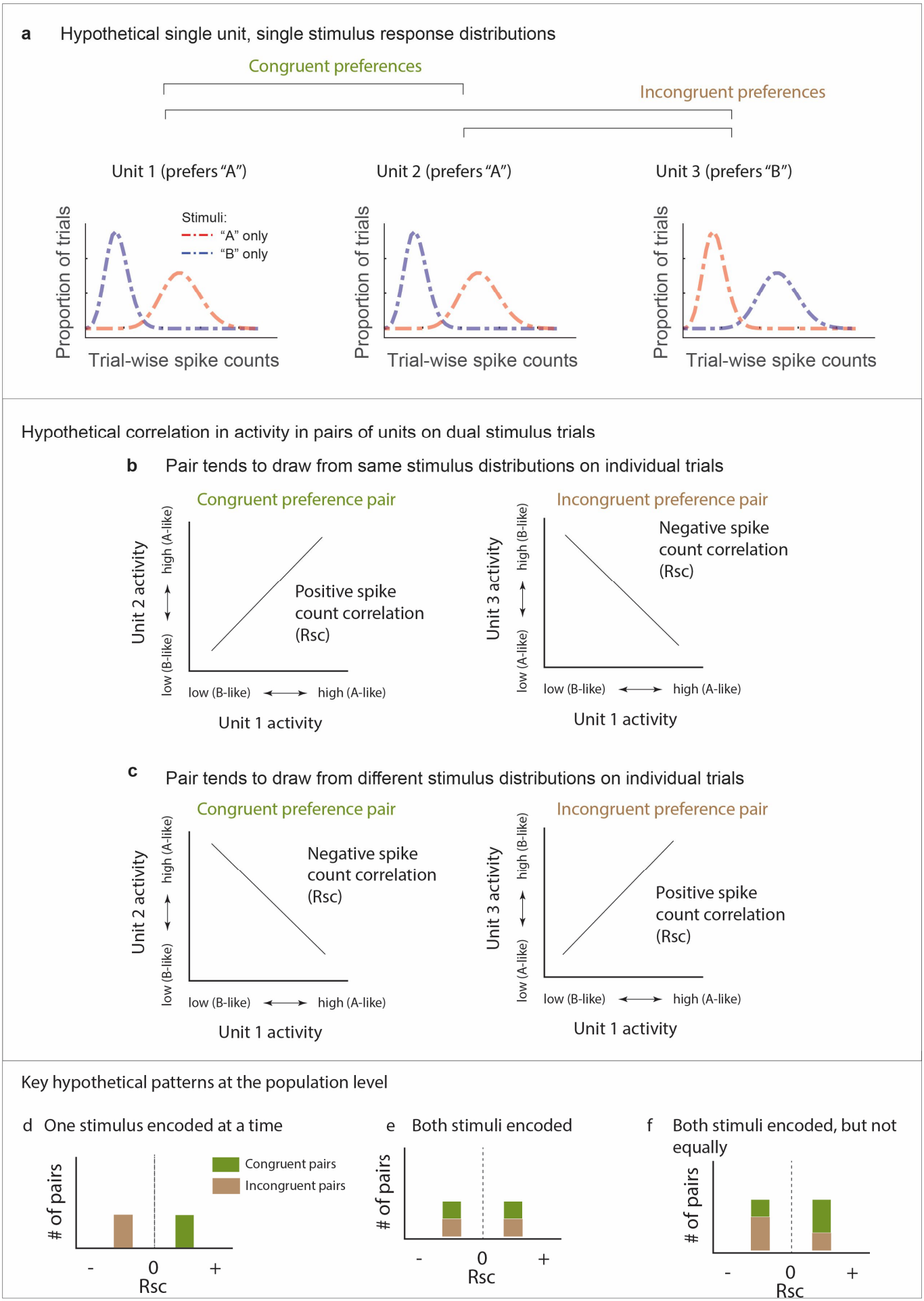
a
Hypothetical single unit, single stimulus response distributions
Congruent preferences
Incongruent preferences
Unit 1 (prefers "A")
Unit 2 (prefers "A")
Unit 3 (prefers "B")
Stimuli:
"A" only
"B" only
Proportion of trials
Trial-wise spike counts
Hypothetical correlation in activity in pairs of units on dual stimulus trials
b
Pair tends to draw from same stimulus distributions on individual trials
Congruent preference pair
Incongruent preference pair
Unit 2 activity
Unit 3 activity
high (A-like)
low (B-like)
high (B-like)
low (A-like)
Positive spike count correlation (Rsc)
Negative spike count correlation (Rsc)
low (B-like)
high (A-like)
Unit 1 activity
c
Pair tends to draw from different stimulus distributions on individual trials
Negative spike count correlation (Rsc)
Positive spike count correlation (Rsc)
Key hypothetical patterns at the population level
d One stimulus encoded at a time
e Both stimuli encoded
f Both stimuli encoded, but not equally
# of pairs
Congruent pairs
Incongruent pairs
-
0
+
Rsc

Figure 3. Schematic depiction of possible response patterns and resulting correlations. A. Three hypothetical neurons and their possible spike count distributions for single stimulus presentations. Unit 1 and Unit 2 both respond better to stimulus "A" than to stimulus "B" ("congruent" preferences). Unit 3 shows the opposite pattern ("incongruent" preferences). B.,C. Possible pairwise spike count correlation (Rsc) patterns for these units. Two units that havecongruent A vs. B response preferences will show positive correlations with each other if they both show "A-like" or "B-like" activity on the same trials (panel B, left). In contrast, if one unit prefers "A" and the other "B" (incongruent), then A-like or B-like activity in both units on the same trial will produce a negative spike count correlation (panel B, right). The opposite pattern applies when units tend to respond to different stimuli on different trials (panel C). D-F. Key examples of the inferences to be drawn at the population level from these potential correlation patterns. D. Positive correlations among "congruent" pairs negative correlations among "incongruent" pairs would suggest only one stimulus is encoded at the population level at a time. E. If both stimuli are encoded in the population, then both positive and negative correlations might be observed among both congruent and incongruent pairs. F. Both stimuli may be encoded, but not necessarily equally. This example shows a pattern intermediate between the illustrations in D and E, and is consistent with one of the two stimuli being overrepresented compared to the other. Other possibilities exist as well, including that neurons may could be uncorrelated with one another (not shown), which would also serve to preserve information about both stimuli at the population level.

Several key potential patterns of spike count correlations across a population of pairs of neurons are illustrated in Figure 3D-F. If the population tends to encode the same stimulus at the same time, then pairs of neurons with congruent preferences will exhibit positive correlations and those with incongruent preferences will exhibit negative correlations (Fig 3D). If the population tends to encode both stimuli, then both positive and negative correlations should occur in both pairs with congruent preferences and pairs with incongruent preferences (Fig. 3E). A third possibility is that both stimuli may be represented at the population level but not evenly so. Such a bias could be reflected by unequal amounts of positive and negative correlations (Fig. 3F).

It should be noted that it is likely that all spike count correlations between pairs of neurons ride on an overall wave of at least slight positivity, due to shared sensitivity to non-stimulus-related factors like overall arousal level or satiety-related signals that might accompany task performance. Thus, the negative- and positive-modes of a broad distribution may not be symmetric around 0 but slightly shifted towards the positive side.

With two objects, distinct distributions of positive and negative spike count correlations occur in V1

We now turn to the actual results with these predictions in mind, starting with the example units illustrated in Figure 2A. Units 1 and 2 exhibited congruent stimulus preferences: stimulus "A", elicited higher spike counts (red line) than stimulus "B" (blue line) for both. Unit 3 had the opposite (incongruent) preference, with higher

spike counts for “B” than for “A”. Figure 4A shows the activity of each of these units on individual “A-and-B” stimulus presentations plotted against the others. The pattern of spike count correlation on individual stimulus presentations varied depending on the stimulus tuning preferences, with the pairing between the units with congruent preferences yielding a positive value (0.56, panel d) and the two pairings involving incongruent preferences yielding negative spike count correlations (-0.45, -0.34, panels e and f). This pattern is borne out when the full set of pairings involving Unit 1 and other units recorded at the same time that also showed “mixture” response patterns is considered (Figure 4B): all the pairings that involved congruent tuning preferences yielded positive correlations, and all of these correlations are individually significant (green bars, $p<0.05$). In contrast, all the pairings that involve incongruent tuning preferences yielded negative correlations (brown bars); as expected, these are slightly more weakly negative than the congruent pairings are positive, but 1 of 5 reaches individual significance (darker brown, $p<0.05$).

We next considered the population level (with each pair of units contributing multiple r_{sc} values to the population distribution, one value for each relevant stimulus condition; see methods for additional details). We first focused on the full set of formally identified “mixtures” subgroup in the adjacent stimulus dataset (Figure 4C), we can see that the pattern observed for the example cells in Figure 2A and 4A holds at the population level: neural pairs in which both units responded better to the same individual stimuli tended to have positive correlations with each other (“congruent preferences”, green bars, median 0.486), whereas those that had different (“incongruent”) stimulus preferences tended to exhibit negative correlations (brown bars, median -0,14). The spread of values is broad, with many of the pairs of “incongruent-preference” neurons in particular exhibiting positive values (a point we will return to in Figure 6).

Because of the lack of an adequate population of “mixture”-classified pairs in the V1 superimposed gratings dataset to compare to the adjacent gratings dataset, we next compared the populations as a whole (Figure 4D, F). The patterns are quite different between these two datasets. In the adjacent-stimulus dataset, the overall broad distribution and distinction between congruent-preference and incongruent-preference subgroups holds even when not selecting for “mixture” fluctuating patterns (green bars vs. brown bars, median r_{sc} 0.252, -0.052). However, this is much less true of the superimposed-gratings dataset (Figure 4F): here, there is very little difference between the congruent-preference and incongruent-preference pairs of neurons (median congruent-preference r_{sc} = 0.159, median incongruent-preference r_{sc} = 0.144), nor is there much difference between the spike count correlations observed on dual-gratings presentations vs. individual grating presentations for this dataset (orange dashed line). In contrast, there is a distinct difference between spike count correlations observed on the dual-stimuli vs. individual-stimulus presentations in the adjacent-stimulus dataset (orange dashed line, Figure 4CD). We verified that this unusual pattern of positive and negative spike count correlations evoked by two objects was not an artifact of multi-unit recordings: Figure 4E shows the spike count correlation patterns observed for the subset of 24 combinations of well-isolated units recorded simultaneously in the adjacent

gratings dataset. While the data is sparse, the overall pattern is consistent with the observations from the full dataset.

We next considered whether this overall pattern was robust to the classification categories emerging from the Bayesian model comparison. While “mixtures” reflect the strongest evidence for activity fluctuations at a stimulus presentation time scale, activity fluctuations are not fully ruled out among “singles” and “intermediates”. For example, if a neuron tended to respond in an “A-like” fashion on a preponderance of trials but in a “B-like” fashion on only a few of them, the Bayesian model classifier will rate “single” as more likely than “mixture” even though there is some evidence of fluctuation. Relatedly, if a neuron tended to switch between A-like and B-like response patterns more rapidly than the 200 ms stimulus presentation time scale, its overall response pattern would be best described as “Intermediate”. Thus, one might expect the general pattern observed among “mixtures” to also be present to a lesser degree in these other model categories.

Indeed, this is the case. Figure 5 illustrates the median spike count correlation by model classification category, for “congruent-preference” and “incongruent-preference” pairs of neurons. We excluded the “outside” category from this analysis as there were too few units that were classified as such. We found that all 9 combinations of classifications yielded positive median spike count correlations among “congruent” preference pairs and negative correlations among “incongruent” preference pairs. Thus, the overall pattern of results described above does not rest critically on the particular details of the model comparison we implemented here, and is present even among units that could not be formally shown to be fluctuating fully between “A”-like and “B”-like response distributions.

Returning to the predictions laid out in Figure 3D-F, the implication of congruent-preference units being on average positively correlated and incongruent-preference units being on average negatively correlated from a coding perspective is that V1’s representation (among “mixture” units) may be slightly biased towards one or the other stimulus on each individual stimulus presentation, most closely resembling the schematic depiction in Figure 3D. However, the actual data involves a broad distribution with positive spike count correlations also occurring among the incongruent-preference pairs and negative spike count correlations among the congruent-preference pairs. Overall, this is most consistent with the schematic depiction in Figure 3F. In short, while the overall pattern of activity among “mixture” units is biased towards one stimulus over the other on individual stimulus presentations, there are ample cases of units that do not follow this pattern, and these exceptions may be sufficient to preserve information about the other stimulus on any given trial.

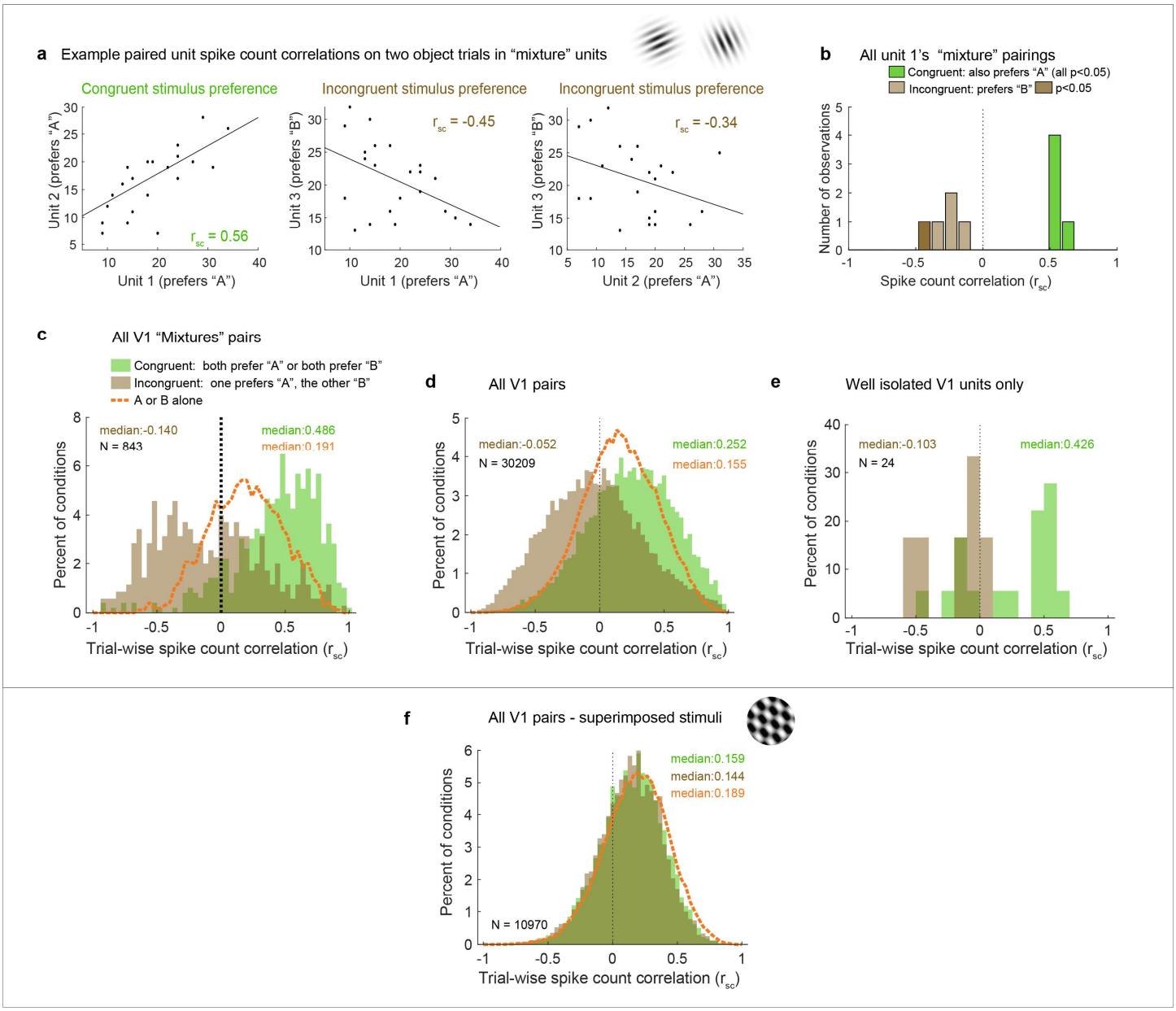

Figure 4. Patterns of spike count correlations among pairs of V1 neurons in different subgroups and conditions. A. Example units' correlation patterns (same units as Figure 2A). The two units that shared a similar tuning preference ("congruent") exhibited positively correlated spike count variation on individual stimulus presentations for the dual stimulus condition (left), whereas both Unit 1 and Unit 2 exhibited a negative correlation with the differently-tuned ("incongruent") Unit 3 (middle and right panels). B. Distribution of R_{sc} values for the other units that were simultaneously recorded with Unit 1 and were also classified as "mixtures", color coded according to whether the stimulus preference of the other unit was the same as that of Unit 1 ("congruent", green) or different ("incongruent", brown). All of the "congruent" pairs exhibited positive correlations, and 5 of 5 were individually significant (p<0.05). All of the "incongruent" pairs exhibited negative correlations, and 1 of 5 was individually significant (p<0.05). C. Overall, neural pairs in which both units met the "mixture" classification showed distinct positive and negative patterns of correlation in response to adjacent stimuli. Positive correlations were more likely to occur among pairs of neurons that responded more strongly to the same individual stimuli ("congruent", green bars, median r_{sc} = 0.486), and negative correlations were more likely to occur among pairs of neurons that responded more strongly to different individual stimuli ("incongruent",brown bars, median r_{sc} = -0.14, p<0.0001, see Methods). This bimodal distribution did not occur when only a single

stimulus was presented (dashed orange line). D, E. This pattern of results held even when all the unit pairs were considered in aggregate (D, "congruent preference" pairs, median r_{sc} = 0.252; "incongruent preference" pairs, median r_{sc} = -0.052, p<0.0001), and also occurred for well-isolated single units (E). F. However, among pairs recorded during presentation of superimposed gratings, this pattern was not apparent: unit pairs tended to show positive correlations in both cases ("congruent preference" median r_{sc} =0.159, "incongruent preference" median r_{sc} = 0.144), and there was little evident difference compared to when a single grating was presented (orange line). See Supplementary Table for additional information.

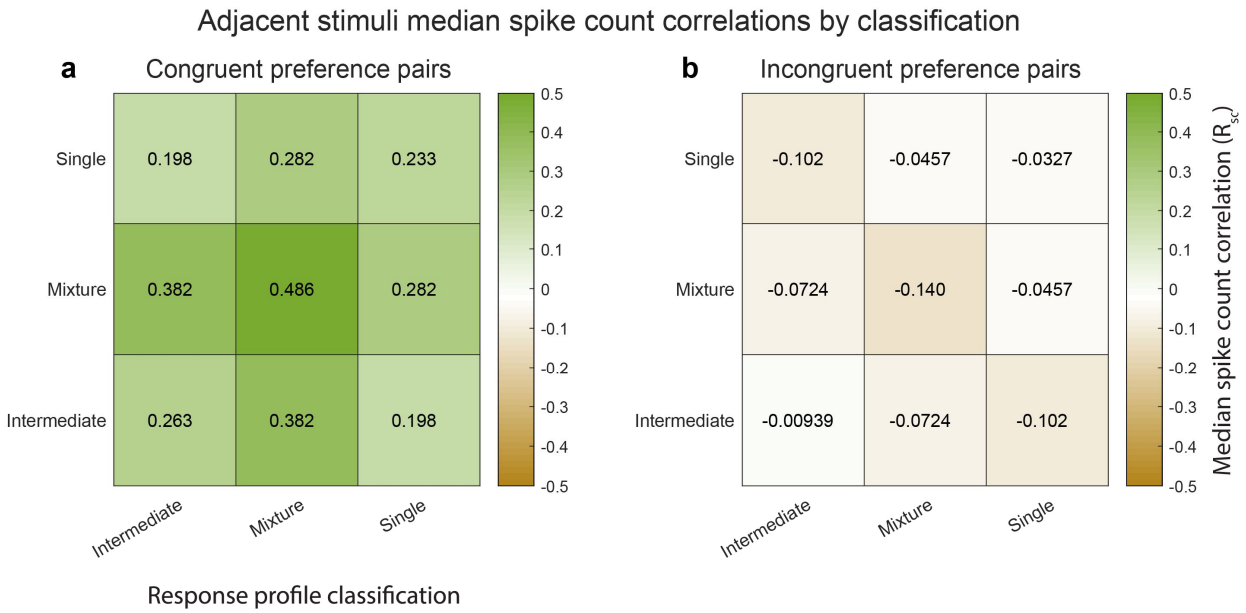

Figure 5. Median spike count correlations as a function of congruent-incongruent preference (panel a vs. panel b) and as a function of the response profile classification resulting from the Bayesian model comparison for the adjacent stimulus dataset. The "mixture"-"mixture" combinations produced the strongest positive (congruent preference pairs) and strongest negative (incongruent preference pairs) median spike count correlations, but all other combinations also involved positive median correlations for congruent preference pairs and negative median correlations for incongruent preference pairs. See Supplementary Table for additional information.

To visualize this in another way, we repeated the calculation of Pearson's correlations between pairs of unit-conditions classified as mixtures using not the spike counts on each stimulus presentation but an assignment score concerning how "A"-like vs "B"-like the spike count was on an individual stimulus presentation (ranging from 0 to 1; see methods). Plotted this way, a positive correlation indicates that the two units in the pair tended to exhibit response patterns consistent with the same object at the same time, whereas a negative correlation

indicates that the two units tended to exhibit responses consistent with different objects at the same time. The overall pattern in the data is positively skewed (Figure 6), but with a long tail on the negative side, consistent with the population of units giving an edge to one stimulus over the other on each individual presentation, but not to the complete exclusion of the other stimulus.

We note that this correlation pattern cannot be accounted for by any obvious confounds. As mentioned previously, all stimulus presentations with microsaccades were excluded from the analyses, limiting the degree to which shared dependence on eye movements could affect the correlation patterns. Furthermore, any variability in fixation position across stimulus presentations might affect the assessment of spike count correlations within a particular pair of neurons, but would not be expected to produce (a) a bimodal distribution of spike count correlations at the population level, that (b) occurs especially strongly when two distinct objects are presented. For example, if variability in fixation caused positive correlations between pairs of neurons whose receptive fields were aligned (likely at most a very small subset of our data), this effect should be equally present on both single stimulus presentations when the stimulus is in those receptive fields and on double stimulus presentations. Yet, as can be seen in Fig 5 C,D, the positive extent of the correlations on double stimulus presentations among “congruent preference” pairs is higher than is observed on single stimulus presentations (green bars extend to higher values than the orange curve), and vice versa for the “incongruent preference” pairs.

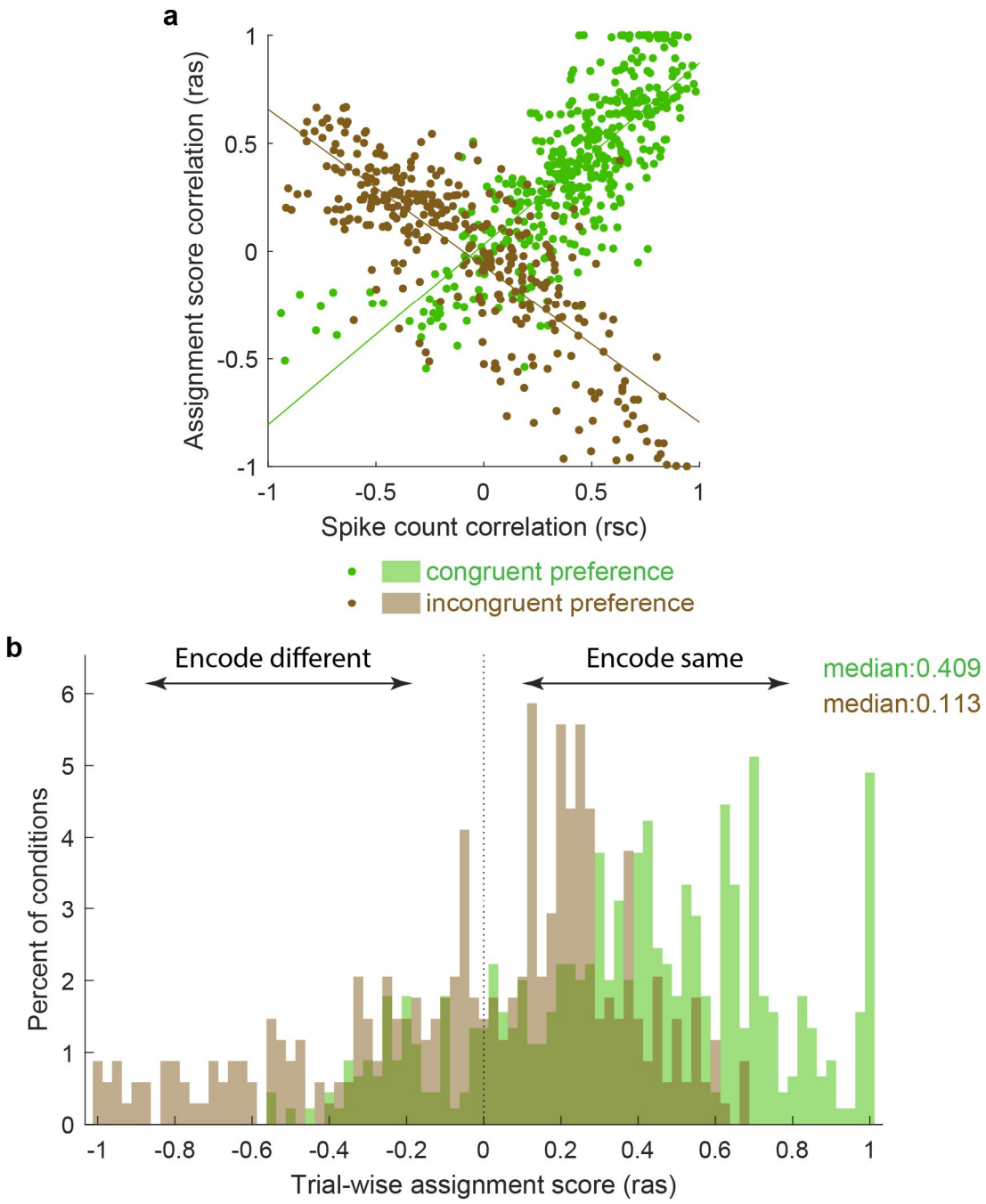

Figure 6. Activity fluctuations in "mixture" pairs of unit-conditions are consistent with a bias towards both units in the pair tending to signal the same stimulus at the same time. This analysis involved the Pearson's correlation coefficients computed on assignments scores (r_{as}), which take into account whether the response on combined "AB" stimulus presentations is more "A-like" vs. "B-like". For two units that share a similar preference (e.g both respond better to A or both respond better to B), this correlation will have the same sign as the spike count correlation (panel a, green points, positively sloped best fit line). For two units that prefer different stimuli, this correlation will be opposite in sign to the spike count correlation (panel a, brown points, negatively sloped best fit line). The overall positive skew in the assignment score correlations for both the "same" and "different" preferring unit-condition pairs (panel b) therefore indicates a bias for the same stimulus at the same time. The negative tail indicates the other stimulus is nevertheless also represented in a (smaller) subpopulation of neurons.

With two objects, distinct distributions of spike count correlations occur in V4

We next assessed V4, which showed both similarities and differences in comparison to V1. Like V1, activity patterns differed considerably in the superimposed vs. adjacent stimuli cases. However, the details of these differences differed: while "mixtures" were present in both the superimposed and adjacent stimulus conditions in V4, "intermediates" were more prevalent in the adjacent stimulus case than in the superimposed stimulus case. Given that "intermediates" could also reflect fluctuations (like "mixtures" but on a faster-than-stimulus-presentation time scale), we considered both mixtures and intermediates as subcategories of particular interest for the V4 dataset (Figure 7).

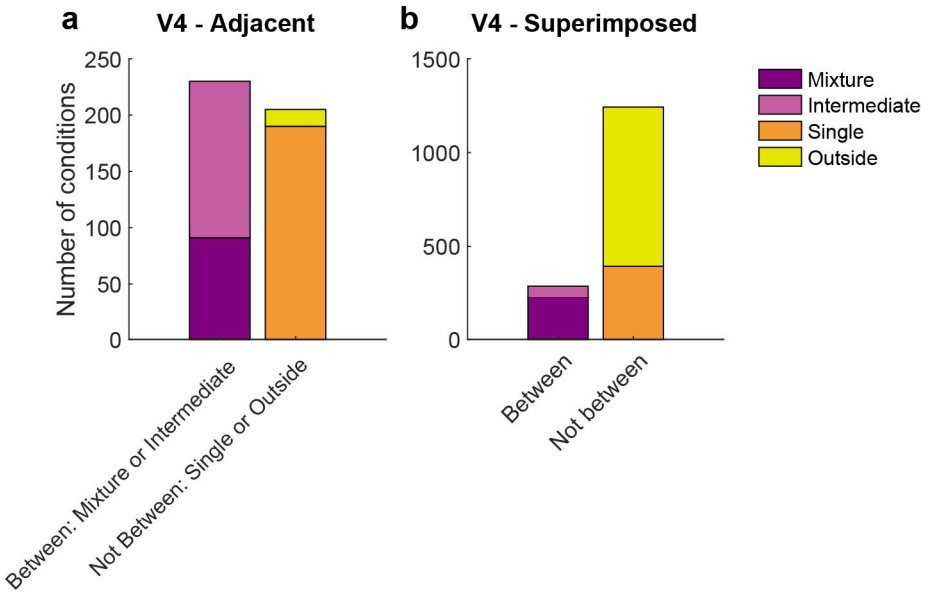

Figure 7. Results of the response pattern classification analysis for V4 units. Shown here are classifications for all units regardless of confidence level, and results from gabors and natural images are combined. See Supplementary Figure 5 for a breakdown by confidence level and for gabors and natural images separately. "Mixtures" were seen in both datasets, but "Intermediates" were seen primarily in the adjacent-stimulus dataset. These two categories can in principle both contain fluctuating activity, and are grouped here as "between" (i.e. the average response for dual stimuli for these two categories is between the average responses to single stimuli). As with V1, the relative proportions of "singles" vs "outsides" also differed across these datasets. The combined incidence of these "not between" categories was higher for the superimposed dataset than for the adjacent dataset.

The patterns of spike count correlations across mixture-mixture pairs in V4 varied considerably based on whether the stimuli were adjacent vs. superimposed and, for adjacent stimuli, whether the two units in the pair exhibited the same or different stimulus preferences (Figure 8). For adjacent mixture-mixture pairs (Panel A), the same-preferring units again tended to show positive spike count correlations, whereas for different-preferring pairs, the distribution appeared centered around zero. It is unclear whether these pairs are truly uncorrelated or if they

might appear uncorrelated due to a negative, stimulus-related, correlation being cancelled out by a comparable, globally shared positive correlation that could stem from other factors (e.g. shared reward sensitivity). When intermediate-intermediate patterns are included, the overall pattern of a difference between the same-preferring and different-preferring distributions is preserved (panel B), although now the different-preference pairs are slightly positive. This pattern was still present when no selection for response pattern was applied (panel C), and is perhaps best appreciated by comparing the medians of the distributions (Figure 8f): there is a distinct difference between the median spike count correlation for same-preference and different-preference pairs for the adjacent dataset. Similar differences in the correlation patterns of same-preference vs different-preference pairs have also been identified in a previous study involving responses of V4 neurons to adjacent gratings (Verhoef and Maunsell, 2017).

However, again like V1, when the two stimuli were presented in a superimposed fashion, this difference was no longer evident. This was the case across the whole dataset (Figure 8e-f) as well as for mixture-mixture pairs (Figure 8d,f), suggesting that when fluctuations do occur for superimposed/bound stimuli, they likely reflect a somewhat different underlying mechanism or purpose than when distinct stimuli are presented.

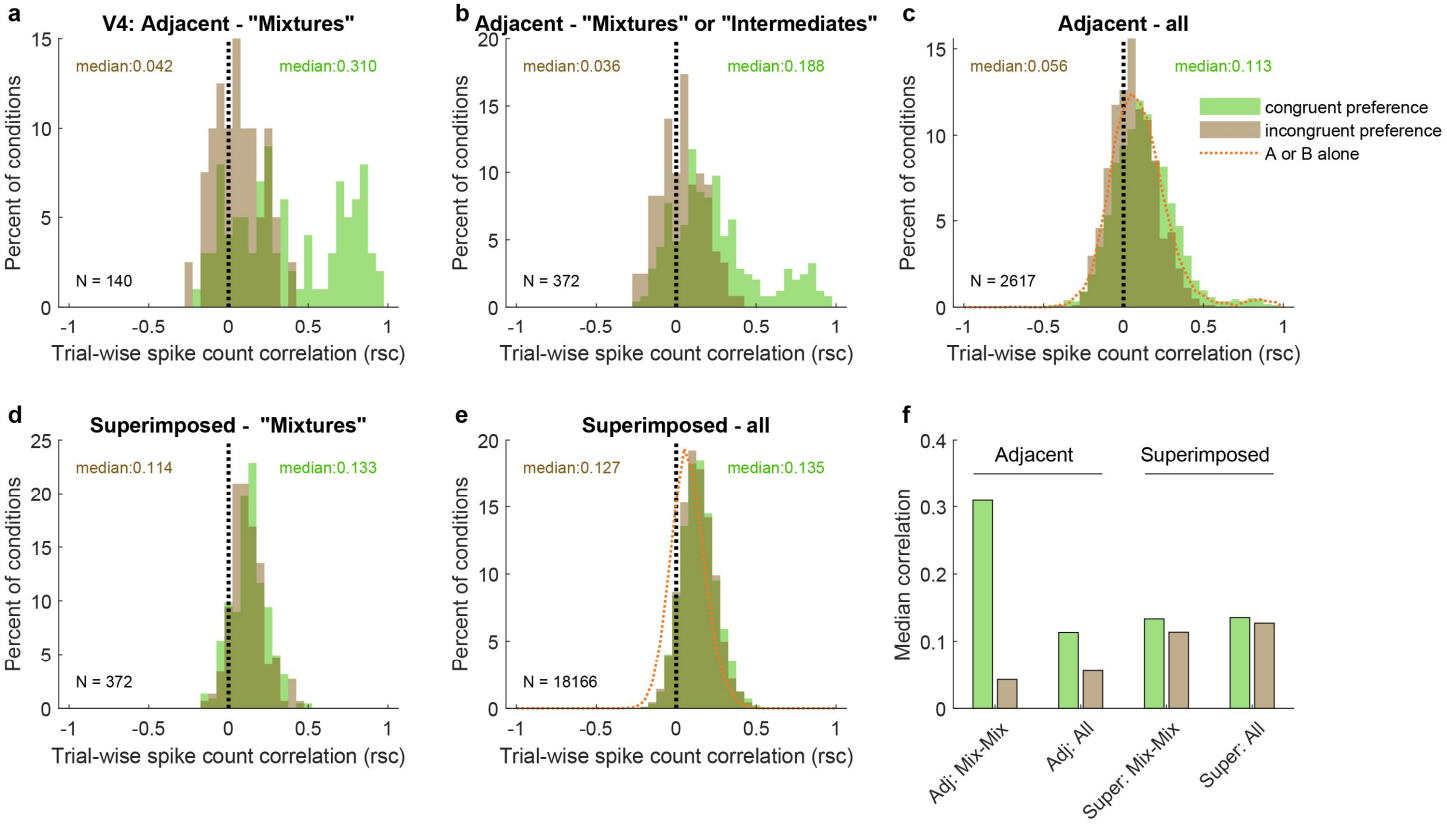

Figure 8. Like V1, pairs of V4 units show different patterns of spike count correlations when there are two adjacent stimuli vs. when there is one superimposed stimulus, depending on the tuning preferences of the pair. A. Mixture-mixture pairs for adjacent stimuli (gabors or images), color coded by whether the two units in the pair shared the same or had different tuning preferences. The "congruent preference" and "incongruent preference"

median correlations differed (p<0.002, see Methods). B. Similar but including intermediate-intermediate pairs, since they too may be fluctuating (median difference p<0.0001). C. All unit pairs tested with adjacent stimuli, regardless of classification in the modeling analysis (median difference p<0.0001). Orange line shows the results for single stimulus presentations. D. Similar to A but for superimposed stimuli (median difference not significant). E. Similar to C but for superimposed stimuli (median difference not significant). F. Comparison of median spike count correlations in the adjacent vs. superimposed datasets, color coded by tuning preference.

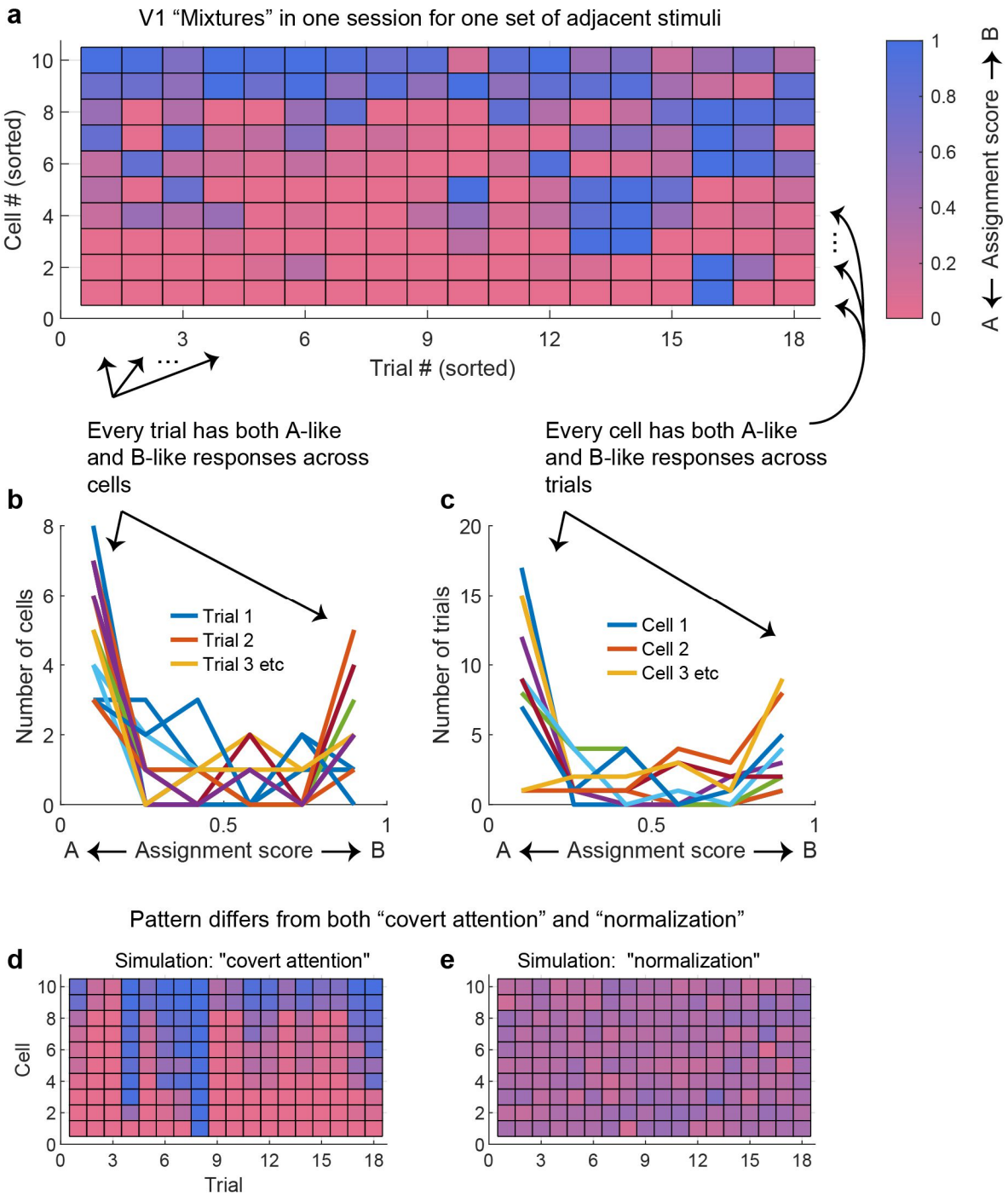

Figure 9. At the population level, each stimulus appears to be encoded by at least some units on every trial. A. The activity of 10 simultaneously recorded V1 units on 18 trials in which a particular combination of two adjacent gratings were presented. The activity of each unit was color-coded according to how "A-like" (red) or "B-like (blue) the responses were on that trial. Only units for which "mixture" was the best descriptor of their response patterns are shown (winning probability > 0.5, indicating "mixture" was at least as likely as all other possibilities combined). There are both red and blue squares in every row, supporting the interpretation that these cells exhibited fluctuations across trials. There are also red and blue squares in every column, indicating that on every trial some cells were responding in an "A-like" fashion and others in a "B-like" fashion. B. Histogram of the number of cells responding in "A-like", "B-like", or intermediate levels on each trial (each trace is a separate trial). C. Similar histogram, but indicating the number of trials in which each cell responded in an "A-like", "B-like", or intermediate firing pattern. D. A simulation of the expected pattern if the observed fluctuations chiefly involved covert fluctuations of attention – cells would be expected to show strong correlations with each other and respond in "A-like" or "B-like" fashion on the same trials. This simulation was constructed by retaining the cell identity and sets of responses observed for each cell, then instituting a strong correlation between them and shuffling the trials in random order. E. A simulation of the expected pattern if cells were not fluctuating but instead averaging their inputs. This simulation was constructed by assuming that each trial's response represented a draw from a normal distribution with the same mean as the observed distribution (0.34) and a standard deviation of 0.10.

The preceding spike count correlation analyses captures correlations as a single correlation value per pair of units. This approach is necessary for population-level statistical comparisons and comparison with similar published values in the literature. Reassuringly, the general findings from this approach can also be observed when considering the pattern of responses in a larger set of simultaneously recorded units across individual trials within individual recording sessions. Figure 9A shows the results from an individual recording session involving V1 units responding to pairs of adjacent stimuli. Ten units that exhibited "mixture" response patterns to a particular set of stimuli are shown, with their activity illustrated in color across the 18 trials involving those stimuli. Key observations from this figure match the observations presented previously: 1) individual units show both "A-like" and "B-like" (red and blue) response patterns across trials – as expected since we selected "mixture" units to include in the plot; 2) pairs of units can show correlations with each other (e.g., units 1 and 2 show strongly positively correlated fluctuation patterns, and units 3-5 show positive correlations that are present but somewhat weaker. However, this figure also makes clear that simultaneously recorded units do not correlate perfectly – there is considerable independence in what individual units are doing (compare, for example, units 3-5 with units 1 & 2). The net result of this is that on individual trials, some units across the population are responding in an A-like fashion and others are responding in a B-like fashion. Figures 9BC quantify this in a different way – at the cell level and at the trial level, individual cells exhibit some A-like and some B-like responses (as baked in by the selection criteria Figure 9C), and on individual trials, some cells exhibit A-like and others B-like responses (Figure 9B). This supports our overall interpretation that, at the population level, information about both stimuli is preserved on individual trials.

Figures 9DE illustrate how very different these observed patterns are from two *a priori* alternative possibilities that would involve loss of information about the two stimuli at the population level. Figure 9D captures what one might expect if fluctuations were due to covert shifts of attention – in this case, there might

have been strongly correlated fluctuations in activity across all the neurons in the population, not merely individual pairs or small groups. This would appear as vertical stripes of shared blue or shared red across the neural population, indicating that only one stimulus was being encoded at a time. Figure 9E captures what one might expect if neurons were not fluctuating at all, but responding to combinations of stimuli by exhibiting normalized or averaged responses intermediate between the responses evoked by either stimulus along – a relatively uniform purple pattern across the neural population. In short, the pattern of responses we observed is quite different from these two alternative "lossy" possibilities.

Discussion

The central observations in this paper are twofold. First, we identified fluctuating activity patterns in V1, evoked only by combinations of stimuli that are parsed as separate objects. These fluctuations were formally identified using a statistical analysis method benchmarked to the response patterns evoked by each of the stimuli independently (Caruso et al., 2018; Mohl et al., 2020; Glynn et al., 2021). This finding suggests not only that multiplexing of information may be a general characteristic of sensory signals in the brain, but also implicates it in the process of separating vs. grouping of stimuli into objects.

These findings laid the groundwork for our second major question, how fluctuating activity patterns are coordinated across neurons and the implications for coding of stimuli at the population level. We found patterns of spike count correlations that differed substantially from those observed previously, but only when two objects were presented. Single objects (whether individual gratings or two superimposed gratings) yielded correlation patterns very similar to previous reports in the literature (Cohen and Kohn, 2011; Ruff et al., 2016; Ruff and Cohen, 2016), and the correlations did not greatly depend on whether the two units in the pair preferred the same individual stimulus or different ones. In contrast, when two stimuli were presented adjacent to one another other, two distinct distributions emerged based on whether the two units in the pair preferred the same individual stimulus (associated with generally positive spike count correlations) vs different individual stimuli (associated with generally negative spike count correlations in V1 or simply less positive spike count correlations in V4). This pattern was observed in the population as a whole, but was especially pronounced in the subset of units that exhibited "mixture"-type response patterns indicating fluctuating across stimulus presentations between the response distributions associated with each of the individual stimuli.

We interpret these observations under the conceptual framework of the challenge that visual cortex faces when representing a visual scene that contains either individual stimuli, combinations of stimuli that bind to form one object, or combinations of stimuli that remain perceptually distinct from each other. The pattern of positive and

negative (or less positive) correlations exhibited between pairs of such units is consistent with a population code biased towards one of the two stimuli on any given stimulus presentation, but that preserves information about the other stimulus as well.

It is interesting to note that we observed evidence of multiplexing each stimulus even in V1 where receptive fields are small and the stimuli we used did not themselves typically span more than one receptive field – thus the coarseness of tuning did not necessarily pose a problem for the encoding of these particular stimuli in this particular brain area. However, the precision of V1's spatial code may not be the limiting factor. Multiplexing is likely to have some as yet unknown characteristic spatial scale that may be determined by the coarsest tuning evident at any stage in the sensory pathway. Future work in which stimuli are systematically varied to manipulate the amount of overlap in the activity patterns evoked in different brain areas by each stimulus alone are needed to answer this question.

The constellation of our findings cannot be easily explained by any obvious alternative explanations. For example, could our focus on the activity patterns of multi-unit clusters have impacted the results? If anything, this would be expected to work against the sensitivity of the analyses, if such clusters consisted of individual neurons who were behaving differently from one another. In fact, our findings were broadly similar in the subset of the data that involved well-isolated single units as compared to the full dataset involving multiunit activity. Furthermore, our previous study identifying coding fluctuations in the inferior colliculus and the MF face patch of inferotemporal cortex was conducted on well-isolated single units (Caruso et al., 2018). Thus, it seems unlikely that single vs multi-unit isolation significantly impacted our findings.

Could either microsaccades or small differences in the fixation position across trials have impacted the results? As noted earlier, we excluded trials with microsaccades, so such small eye movements are unlikely to have affected the findings, and fixational scatter did not vary by stimulus conditions (Supplementary Figure 2). Thus it is unlikely that variation in fixation position contributed to the difference we observed between two-object vs fused-object response patterns or the differences between congruent-preference and incongruent-preference pairs of units. Furthermore, as noted above, we observed similar coding fluctuations in two brain areas (the IC and MF face patch) for auditory and large visual stimuli – i.e. stimulus conditions that are thought to involve less sensitivity to differences in fixation position than V1 and V4 (Bremmer, 2000; Groh et al., 2001; Porter et al., 2006, 2007; Lehky et al., 2008; Maier and Groh, 2010; Bulkin and Groh, 2012b, a; Merriam et al., 2013; Caruso et al., 2018).

Finally, there is precedent in the literature for differences in the spike count correlation patterns of congruent vs. incongruent-preference pairs: a previous study in V4 (Verhoef and Maunsell, 2017) also reported such correlation differences. The general effect size of our V4 results seems to be similar to theirs, particularly when

considering the most comparable conditions. The Verhoef and Maunsell study was not designed to identify coding fluctuations, so the most comparable point of comparison in our study would be the pooled results across all model categories (Fig 8A). Our analysis focused on units with well separated responses to the individual stimuli, which is most comparable to the right side of their Fig 2C; our unit pairs were classified categorically as congruent- or incongruent-preferring rather than on a sliding scale, so it is not immediately apparent how to relate the two studies in that dimension (y axis in their 2C). Nevertheless, the approximate difference between the median or mean congruent-preferring vs. incongruent-preferring correlations is reassuringly similar at about 0.06 in our study and a maximum of about 0.12 in theirs. This suggests that the same-preference vs different-preference correlation patterns observed in the two studies are likely to generalize across different experimental designs.

There has been a rich literature concerning the implications of correlated activity between visually-responsive neurons in recent decades. One school of thought considers correlations in the context of the variability of neural firing. Under this "noise correlation" view, positive correlations have historically been seen as detrimental for encoding information at the population level (Shadlen and Newsome, 1994; Zohary et al., 1994). Such views have also seen notable refinement and qualification since these early studies (Romo et al., 2003; Averbeck and Lee, 2004; Averbeck et al., 2006; Moreno-Bote et al., 2014; Kanitscheider et al., 2015; Kohn et al., 2016; Nogueira et al., 2020; Kafashan et al., 2021) Arguably closer to the current work is a different school of thought, the temporal correlation hypothesis (Milner, 1974; Gray and Singer, 1989; Von Der Malsburg, 1994; Singer and Gray, 1995; Gray, 1999). This theory focused on the need to connect the brain's representation of different attributes of a given object together, and proposed that such binding might be mediated through precise synchrony of spikes among neurons responding to the same object. This view, then, sees correlated activity as both useful and specifically relevant to object vision. Studies exploring this hypothesis have, however, primarily focused on within-trial temporal synchrony of spikes on the order of milliseconds, whereas the noise correlation literature has focused on spike counts in the domain of hundreds of milliseconds and analysis at the level of the ensemble of trials or stimulus presentations. By evaluating spike-count variation at the level of stimulus presentations and comparing the results as a function of the number of stimuli/objects, the present work forges a bridge between these two areas of the literature.

Our findings also suggest re-consideration of two other key processes in visual neuroscience: selective attention and normalization. Selective attention refers to the fact that perceptual awareness is not equal across all stimuli present in a sensory scene. Selective attention can be controlled through "top-down" means, such as via tasks in which participants are cued to focus on one stimulus and ignore others. Indeed, the monkeys were performing just such a task in our adjacent V1 dataset, and thus were in theory ignoring the stimuli whose responses we studied here. But even with correct task performance, top down control of attention is imperfect. Might the fluctuating responses we observed be due to covert shifts of attention from one of the supposedly unattended

stimuli to the other (which could contribute to the observed activity patterns (Ecker et al., 2016; Engel et al., 2016; Denfield et al., 2018))? We think not. If this were the case, then the neurons should have fluctuated in more perfect harmony with one another. As shown quantitatively in Figure 6 and qualitatively in Figure 9, although there is a bias in which stimulus is "capturing" the response patterns on individual trials, there remains a substantial portion of the neural population that is responding to the other stimulus. And the observed pattern of fluctuating activity is very different from a simulation of covert attention (Figure 9A vs. 9D). While further work on this question is needed, we think it is worth noting that the patterns of activity that we observed can in principle support preservation of information about all stimuli in the scene. Processes involved in selective attention might contribute to the creation of biases within this representation, or could act at later stages on the information preserved within these representations to enhance awareness of one or more of the represented stimuli.

Previous findings from the existing literature on attention and related areas are consistent with this new view, and could easily be evaluated anew using the approach we described here. Trial-averaged neural responses to attended and unattended stimuli can often be modeled as a weighted combination of the responses to those stimuli when presented alone (Boynton, 2009; Lee and Maunsell, 2009; Reynolds and Heeger, 2009; Ni et al., 2012; Ni and Maunsell, 2017; Verhoef and Maunsell, 2017; Ni and Maunsell, 2019) (Lee and Maunsell, 2009; Ni et al., 2012; Ni and Maunsell, 2017; Verhoef and Maunsell, 2017; Ni and Maunsell, 2019). Such averaging responses are seen not only in attention paradigms but in other contexts as well (e.g. (see also Xiao et al., 2014; Xiao and Huang, 2015)) and are generally referred to as normalization. Importantly, these reports have concerned responses pooled across trials. Trial-wise spike count distribution models such as those used here and/or faster sub-trial analyses such as those we have introduced in previous work (Caruso et al., 2018; Glynn et al., 2021) might indicate that such apparently averaging responses actually indicate fluctuations occurring on either the stimulus presentation or sub-stimulus presentation time scales, and not a true stable average (e.g. Figure 9A vs 9E).

Recent work suggests another more perceptual tie between studies of attention and the findings we report here. The likelihood of detecting a brief near-threshold visual stimulus varies with the phase of the brain wave oscillations at the time the stimulus is presented (Busch et al., 2009; Busch and VanRullen, 2010; Vanrullen et al., 2011; Fiebelkorn et al., 2013; Fiebelkorn et al., 2018; Helfrich et al., 2018; Fiebelkorn and Kastner, 2019) (see also Engel et al., 2016). This might reflect a perceptual consequence of a brain mechanism in which neurons are slightly biased towards representing some stimuli in the visual scene over others in a naturally-occurring oscillatory fashion. Such bias was evident in the responses observed here, although we did not deploy a task to assess any potential connection to behavior. In our previous study (Caruso et al., 2018), we found that the LFP signal prior to stimulus onset was predictive of whether neurons would "pick" A vs. B on a given trial. Future work will be needed to ascertain whether a similar phenomenon occurs in V1 or V4.

Finally, it is worth noting here that considering how the brain preserves information about *two* visual stimuli presented is still a far cry from understanding how the myriad details present in a natural scene are encoded. When the number of objects gets too great, it is unlikely that neurons can fluctuate between all of them, and this is likely to have consequences for perception, perhaps accounting for well-known limits on the number of objects we can perceive, attend to and remember (e.g. Miller, 1956; Whitney and Levi, 2011; Henry and Kohn, 2020). Future studies incorporating many stimuli and investigating how this changes the pattern of fluctuating activity and correlations between units are needed to shed light on how our brains operate outside the rarefied environment of the laboratory.

Methods

Electrophysiological recordings and visual stimuli

The full experimental procedures are described in Ruff et al.(2016) and Ruff & Cohen (2016) and summarized below. All animal procedures were approved by the Institutional Animal Care and Use Committees of the University of Pittsburgh and Carnegie Mellon University. Each of the data sets consisted of multielectrode recordings from two adult male rhesus monkeys for each brain area (Table 1-2). Recordings were made using chronically implanted a 10 x 10 microelectrode arrays (Blackrock Microsystems) in V1 and and 6 x 8 arrays in V4 (Figure 1A). The electrode shafts were 1mm long, and the minimum distance between the nearest electrodes was 400 μm. In some sessions, recordings were also made using other electrodes in areas MT and 7a, but these data are not included in the current analyses.

The visual stimuli and behavioral experiment for the superimposed stimulus dataset are fully described in Ruff et al.(2016). Monkeys were rewarded for passively viewing individual or superimposed orthogonal drifting gratings, positioned to span the receptive fields of the entire population of neurons under study (size range: 2.5-7°). As noted above, the fixation windows were +/- 0.5 degrees horizontally and vertically, and stimulus presentations with microsaccades (defined as eye velocity exceeding 6 standard deviations above the mean velocity observed during steady fixation, (Engbert and Kliegl, 2003)) were excluded from further analysis. In the full dataset, multiple contrast levels were presented, most of which were not included for analysis in the present study. Here, we included trials in which one grating had a contrast of 0 (i.e. was not visible) and the other had a contrast of 0.5 (“A”-alone and “B”-alone cases) or both gratings had a contrast of 0.5 (“AB”). In most sessions, each stimulus lasted for 200 ms; a few sessions with 1000 ms stimuli were also included but only the first 200 ms were analyzed, i.e. spikes were counted in a 200 ms window after stimulus onset for all the analyses in this study. This spike counting window was offset by the typical response latency for the region under study, i.e. 30-230 ms for V1 and 50-250 ms for V4.

The visual stimuli and behavioral experiment for the V1 adjacent stimulus dataset are fully described in (Ruff and Cohen, 2016). The animals performed a motion direction change detection task in which they were cued in blocks of trials to attend to small drifting Gabor patches (~1°) in various locations and respond when the orientation of the attended location changed. In the current study, we analyzed trials in which attention was directed to a Gabor patch located in the hemisphere ipsilateral to the recorded V1 neurons (i.e. well away from those neurons' receptive fields, see below). On these trials, two unattended Gabor patches were presented in close proximity to each other within the area covered by the receptive fields of the recorded V1 neurons – these receptive fields were approximately 3 degrees eccentric and had classical receptive field diameters typically estimated to be <1 degree of visual angle. These patches were centered 2.5-3.5 degrees eccentrically and each stimulus typically subtended 1 degree of visual angle (see Ruff and Cohen 2016 Fig 1B for a sketch, reproduced here in Supplementary Figure 1). The patches had the same orientation but drifted in opposite directions and were flashed on for 200 ms and off for 200-400 ms. We analyzed responses to all stimuli before the orientation change, excluding the first stimulus in every trial. Again, only correctly performed trials with no microsaccades during stimulus presentations were included for analysis. As noted previously, monkeys were required to maintain fixation within +/- 0.5 degrees, and typically fixation was more precise than required; see Supplementary Figure 2 for fixational scatter in an example session and across sessions.

The adjacent stimulus dataset for V4 involved two types of stimuli, small drifting Gabor patches as above or natural images of animals or common objects, from (Long et al., 2018). Results for the two types of stimuli were combined for the main analyses presented in this paper (Figures 7 and 8), and are broken out separately in Supplementary Figure 5. The monkeys performed a fixation task.

Analysis of spike count distributions

The full description of the statistical evaluation of spike count distributions on combined stimulus presentations can be found in (Caruso et al., 2018; Mohl et al., 2020). Briefly, we deployed a Bayesian procedure for modeling the distribution of spike counts in response to combined stimuli. Assuming that the spike counts corresponding to condition A and condition B are both Poisson-distributed with the rate parameters λ^A and λ^B respectively (and excluding exceptions, see below), the four hypotheses for the spike count distributions for condition AB consist of:

1. "**single**": A single Poisson distribution $\mathrm{Poi}(\lambda^{AB})$, where λ^{AB} exactly equals either λ^A or λ^B.
2. "**outside**": A single Poisson distribution $\mathrm{Poi}(\lambda^{AB})$, where λ^{AB} lies outside the range between λ^A and λ^B.
3. "**intermediate**": A single Poisson distribution $\mathrm{Poi}(\lambda^{AB})$, where λ^{AB} lies inside the range between λ^A and λ^B.
4. "**mixture**": A mixture of the two single-stimulus distribution with an unknown mixing rate α: $\alpha\ \mathrm{Poi}(\lambda^A) + (1-\alpha)\ \mathrm{Poi}(\lambda^B)$

For each "triplet" or combination of A, B, and AB conditions, the hypothesis with the highest posterior probability was selected, based on the intrinsic Bayes factor (Berger and Pericchi, 1996) and using the equal prior (¼) among the four hypotheses, Jeffrey's prior (Berger and others, 2006) for the Poisson rate parameters, and a uniform prior in [0, 1] for the mixing weight α.

Only the triplets satisfying two exclusion criteria are used: (1) the single-stimulus distributions follow Poisson distributions, and (2) the single-stimulus rate parameters λ^A and λ^B are substantially separated. The first criterion was tested using Monte Carlo p-value calculation for a Chi-square goodness-of-fit test ($p>0.10$), and the second criterion was tested by whether the intrinsic Bayes factor of the model $\lambda^A \neq \lambda^B$ is more than three times higher than that of the model $\lambda^A = \lambda^B$. These exclusion criteria were applied to all the analyses in the paper, even those that did not build specifically on this model classification, to ensure that comparisons between subpopulations of the data were not affected by differences in data selection criteria.

The numbers of trials involved for the different data sets are provided in Table 2. The trial counts were adequate to provide accurate model identification according to our previous simulations. Depending on the separation between λ^A and λ^B, we previously found that model identification accuracy in simulations is high for trial counts as low as 5 "AB" trials, and plateaus near ceiling around "AB" trial counts of about 10 trials and above – i.e. below the mean trial counts available here for all datasets (see Figure 4 of Mohl et al., 2020).

Stimuli	Brain area	Task	Monkeys	Available sessions	Sessions for which at least one triplet was included	Available units	Units for which at least one triplet was included	Triplets passing exclusion criteria for analysis
Adjacent	V1	Attention	ST, BR	16	16	1604	935	1389
	V4	Fixation	BA, HO	17	17	991	274	456
Superimposed	V1	Fixation	ST, BR	25	23	2304	770	1686
	V4	Fixation	JD, SY	21	21	1744	817	1529

Table 1. Summary of included data. Analyses were conducted on "triplets", consisting of a combination of A, B, and AB conditions. If the spikes evoked by the A and B stimuli failed to follow Poisson distributions with substantially separated means, the triplet was excluded from analysis. This table shows the numbers of triplets that survived these exclusion criteria for each brain area and type of stimulus condition (last column), as well as the numbers of monkeys, distinct units, and sessions that they were derived from (columns 5-8).

		Number of "A" and "B" trials				**Number of "AB" trials**			
Stimuli	**Brain area**	**mean**	**std**	**min**	**max**	**mean**	**std**	**min**	**max**
Adjacent	V1	21.0	12.3	6	56	17.8	12.8	6	59
	V4	72.8	30.3	5	136	72.2	30.7	6	132

Superimposed	V1	25.4	15.4	7	74	23.3	12.1	7	64
	V4	131.3	42.0	20	196	184.5	64.6	20	270

Table 2. Trial counts for included sessions. The values reported are calculated for individual recording sessions for which at least one triplet was included for the analysis; the numbers of trials are the same for all simultaneously recorded units within a session. The values for "A" and "B" trials indicate the values for either A or B; that is, there were on average 21 "A" trials and 21 "B" trials for each triplet in the adjacent V1 dataset.

Correlation analysis

We calculated spike count correlations between pairs of units recorded at the same time in the same experiment. The Pearson correlation coefficient was calculated on the spike counts for each presentation of each relevant stimulus combination. Stimulus presentations in which one or both units in the pair exhibited an "outlier" response, i.e. more than 3 standard deviations from the mean, were excluded from the analysis. The spike count correlations for particular unit pairs for different stimulus combinations were included in the population analyses as separate observations and were not averaged together. For example, in the V1 adjacent stimulus dataset, pairs were typically tested with two separate adjacent stimulus combinations, differing in the direction of motion, potentially yielding two values of the spike count correlation (assuming both conditions passed the Poisson and response-separation exclusion criteria noted above). Similarly, V4 neurons tested with different combinations of drifting gabors and/or images contributed values of spike count correlations for each stimulus set to the population.

Congruent or incongruent preference

Preference of a unit for a particular stimulus was determined by higher spike counts. Unit pairs that both exhibited more spikes in response to stimulus A than to B, or both exhibited more spikes in response to stimulus B than to A, were defined as "congruent preference". Unit pairs in which one responded with more spikes to A and the other with more spikes to B were defined as "incongruent preference".

Comparison of distributions of spike count correlations

The medians of the "congruent preference" vs. "incongruent preference" distributions of spike count correlations were statistically compared using Monte Carlo methods in which the same/different preference assignments were randomly shuffled and the medians recalculated 10,000 times. When the true difference between the medians was greater than any of the shuffled versions, the p value can be said to be less than 1/10,000 or 0.0001.

Author Contributions:

Experimental design: DAR, MRC

Data collection: DAR, LEK, BB

Data analysis: NYJ, STT, DAR, JMG

Manuscript preparation: NYJ, JMG

Manuscript editing: NYJ, DAR, STT, MAR, JMG

Authors LEK and BB contributed equally.

References

Adelson EH, Movshon JA (1982) Phenomenal coherence of moving gratings. Nature, Lond 300:523-525.

Alonso J-M, Chen Y (2009) Receptive field. Scholarpedia 4:5393.

Averbeck BB, Lee D (2004) Coding and transmission of information by neural ensembles. Trends Neurosci 27:225-230.

Averbeck BB, Latham PE, Pouget A (2006) Neural correlations, population coding and computation. Nat Rev Neurosci 7:358-366.

Boynton GM (2009) A framework for describing the effects of attention on visual responses. Vision Res 49:1129-1143.

Bremmer F (2000) Eye position effects in macaque area V4. Neuroreport 11:1277-1283.

Bulkin DA, Groh JM (2011) Systematic mapping of the monkey inferior colliculus reveals enhanced low frequency sound representation. J Neurophysiol 105:1785-1797.

Bulkin DA, Groh JM (2012a) Distribution of visual and saccade related information in the monkey inferior colliculus. Front Neural Circuits 6:61.

Bulkin DA, Groh JM (2012b) Distribution of eye position information in the monkey inferior colliculus. J Neurophysiol 107:785-795.

Busch NA, VanRullen R (2010) Spontaneous EEG oscillations reveal periodic sampling of visual attention. Proc Natl Acad Sci U S A 107:16048-16053.

Busch NA, Dubois J, VanRullen R (2009) The phase of ongoing EEG oscillations predicts visual perception. J Neurosci 29:7869-7876.

Busse L, Wade AR, Carandini M (2009) Representation of concurrent stimuli by population activity in visual cortex. Neuron 64:931-942.

Caruso VC, Mohl JT, Glynn C, Lee J, Willett SM, Zaman A, Ebihara AF, Estrada R, Freiwald WA, Tokdar ST, Groh JM (2018) Single neurons may encode simultaneous stimuli by switching between activity patterns. Nature communications 9:2715.

Cohen MR, Kohn A (2011) Measuring and interpreting neuronal correlations. Nat Neurosci 14:811-819.

Denfield GH, Ecker AS, Shinn TJ, Bethge M, Tolias AS (2018) Attentional fluctuations induce shared variability in macaque primary visual cortex. Nature communications 9:2654.

Dow BM, Snyder AZ, Vautin RG, Bauer R (1981) Magnification factor and receptive field size in foveal striate cortex of the monkey. Exp Brain Res 44:213-228.

Ecker AS, Denfield GH, Bethge M, Tolias AS (2016) On the Structure of Neuronal Population Activity under Fluctuations in Attentional State. J Neurosci 36:1775-1789.

Engbert R, Kliegl R (2003) Microsaccades uncover the orientation of covert attention. Vision Res 43:1035-1045.

Engel TA, Steinmetz NA, Gieselmann MA, Thiele A, Moore T, Boahen K (2016) Selective modulation of cortical state during spatial attention. Science 354:1140-1144.

Fiebelkorn IC, Kastner S (2019) A Rhythmic Theory of Attention. Trends Cogn Sci 23:87-101.

Fiebelkorn IC, Saalmann YB, Kastner S (2013) Rhythmic sampling within and between objects despite sustained attention at a cued location. Curr Biol 23:2553-2558.

Fiebelkorn IC, Pinsk MA, Kastner S (2018) A Dynamic Interplay within the Frontoparietal Network Underlies Rhythmic Spatial Attention. Neuron 99:842-853 e848.
Georgopoulos A, Schartz A, Kettner R (1986) Neuronal population coding of movement direction. Science 233:1416-1419.
Glynn C, Tokdar S, Zaman A, Caruso VC, Mohl JT, Willett SM, Groh JM (2021) Analyzing second order stochasticity of neural spiking under stimuli-bundle exposure. Annals of Applied Statistics, arXiv:191104387 15:41-63.
Gray CM (1999) The temporal correlation hypothesis of visual feature integration: still alive and well. Neuron 24:31-47, 111-125.
Gray CM, Singer W (1989) Stimulus-specific neuronal oscillations in orientation columns of cat visual cortex. Proc Natl Acad Sci U S A 86:1698-1702.
Groh JM, Kelly KA, Underhill AM (2003) A monotonic code for sound azimuth in primate inferior colliculus. Journal of Cognitive Neuroscience 15:1217-1231.
Groh JM, Trause AS, Underhill AM, Clark KR, Inati S (2001) Eye position influences auditory responses in primate inferior colliculus. Neuron 29:509-518.
Grothe B, Pecka M, McAlpine D (2010) Mechanisms of sound localization in mammals. Physiol Rev 90:983-1012.
Heeger DJ, Simoncelli EP, Movshon JA (1996) Computational models of cortical visual processing. Proceedings of the National Academy of Sciences of the United States of America 93:623-627.
Helfrich RF, Fiebelkorn IC, Szczepanski SM, Lin JJ, Parvizi J, Knight RT, Kastner S (2018) Neural Mechanisms of Sustained Attention Are Rhythmic. Neuron 99:854-865 e855.
Henry CA, Kohn A (2020) Spatial contextual effects in primary visual cortex limit feature representation under crowding. Nature communications 11:1687.
Higgins NC, Storace DA, Escabi MA, Read HL (2010) Specialization of binaural responses in ventral auditory cortices. J Neurosci 30:14522-14532.
Kafashan M, Jaffe AW, Chettih SN, Nogueira R, Arandia-Romero I, Harvey CD, Moreno-Bote R, Drugowitsch J (2021) Scaling of sensory information in large neural populations shows signatures of information-limiting correlations. Nature communications 12:473.
Kanitscheider I, Coen-Cagli R, Pouget A (2015) Origin of information-limiting noise correlations. Proc Natl Acad Sci U S A 112:E6973-6982.
Keliris GA, Li Q, Papanikolaou A, Logothetis NK, Smirnakis SM (2019) Estimating average single-neuron visual receptive field sizes by fMRI. Proceedings of the National Academy of Sciences 116:6425-6434.
Kohn A, Coen-Cagli R, Kanitscheider I, Pouget A (2016) Correlations and Neuronal Population Information. Annu Rev Neurosci 39:237-256.
Lee C, Rohrer WH, Sparks DL (1988) Population coding of saccadic eye movements by neurons in the superior colliculus. Nature 332:357-360.
Lee J, Maunsell JH (2009) A normalization model of attentional modulation of single unit responses. PLoS One 4:e4651.
Lehky SR, Peng X, McAdams CJ, Sereno AB (2008) Spatial modulation of primate inferotemporal responses by eye position. PLoS One 3:e3492.
Lima B, Singer W, Chen NH, Neuenschwander S (2010) Synchronization dynamics in response to plaid stimuli in monkey V1. Cereb Cortex 20:1556-1573.
Long B, Yu CP, Konkle T (2018) Mid-level visual features underlie the high-level categorical organization of the ventral stream. Proc Natl Acad Sci U S A 115:E9015-E9024.
Maier JX, Groh JM (2010) Comparison of gain-like properties of eye position signals in inferior colliculus versus auditory cortex of primates. Frontiers in Integrative Neuroscience 4:121-132.
McAlpine D, Grothe B (2003) Sound localization and delay lines--do mammals fit the model? Trends Neurosci 26:347-350.
Merriam EP, Gardner JL, Movshon JA, Heeger DJ (2013) Modulation of Visual Responses by Gaze Direction in Human Visual Cortex. The Journal of Neuroscience 33:9879-9889.
Miller GA (1956) The magical number seven, plus or minus two: some limits on our capacity for processing information. Psychological Review 63:81-97.
Milner PM (1974) A model for visual shape recognition. Psychol Rev 81:521-535.

Mohl JT, Caruso VC, Tokdar S, Groh JM (2020) Sensitivity and specificity of a Bayesian single trial analysis for time varying neural signals. Neurons, Theory, Data Analysis, and Behavior.
Moreno-Bote R, Beck J, Kanitscheider I, Pitkow X, Latham P, Pouget A (2014) Information-limiting correlations. Nat Neurosci 17:1410-1417.
Ni AM, Maunsell JHR (2017) Spatially tuned normalization explains attention modulation variance within neurons. J Neurophysiol 118:1903-1913.
Ni AM, Maunsell JHR (2019) Neuronal Effects of Spatial and Feature Attention Differ Due to Normalization. J Neurosci 39:5493-5505.
Ni AM, Ray S, Maunsell JH (2012) Tuned normalization explains the size of attention modulations. Neuron 73:803-813.
Nogueira R, Peltier NE, Anzai A, DeAngelis GC, Martinez-Trujillo J, Moreno-Bote R (2020) The Effects of Population Tuning and Trial-by-Trial Variability on Information Encoding and Behavior. J Neurosci 40:1066-1083.
Palanca BJ, DeAngelis GC (2005) Does neuronal synchrony underlie visual feature grouping? Neuron 46:333-346.
Porter KK, Metzger RR, Groh JM (2006) Representation of eye position in primate inferior colliculus. J Neurophysiol 95:1826-1842.
Porter KK, Metzger RR, Groh JM (2007) Visual- and saccade-related signals in the primate inferior colliculus. Proceedings of the National Academy of Sciences of the United States of America 104:17855-17860.
Reynolds JH, Heeger DJ (2009) The normalization model of attention. Neuron 61:168-185.
Rodman HR, Albright TD (1989) Single-unit analysis of pattern-motion selective properties in the middle temporal visual area (MT). Exp Brain Res 75:53-64.
Romo R, Hernandez A, Zainos A, Salinas E (2003) Correlated neuronal discharges that increase coding efficiency during perceptual discrimination. Neuron 38:649-657.
Ruff DA, Cohen MR (2016) Attention Increases Spike Count Correlations between Visual Cortical Areas. J Neurosci 36:7523-7534.
Ruff DA, Alberts JJ, Cohen MR (2016) Relating normalization to neuronal populations across cortical areas. J Neurophysiol 116:1375-1386.
Shadlen M, Newsome W (1994) Noise, neural codes and cortical organization. **Current Opinion in Neurobiology** 4:569-579.
Singer W, Gray CM (1995) Visual feature integration and the temporal correlation hypothesis. Annu Rev Neurosci 18:555-586.
Vanrullen R, Busch NA, Drewes J, Dubois J (2011) Ongoing EEG Phase as a Trial-by-Trial Predictor of Perceptual and Attentional Variability. Front Psychol 2:60.
Verhoef BE, Maunsell JHR (2017) Attention-related changes in correlated neuronal activity arise from normalization mechanisms. Nat Neurosci 20:969-977.
Von Der Malsburg C (1994) The correlation theory of brain function. In: Models of neural networks, pp 95-119: Springer.
Werner-Reiss U, Groh JM (2008) A rate code for sound azimuth in monkey auditory cortex: implications for human neuroimaging studies. J Neurosci 28:3747-3758.
Whitney D, Levi DM (2011) Visual crowding: a fundamental limit on conscious perception and object recognition. Trends Cogn Sci 15:160-168.
Willett SM, Groh JM (2022) Multiple sounds degrade the frequency representation in monkey inferior colliculus. Eur J Neurosci 55:528-548.
Woods TM, Su TK, Recanzone GH (2001) Spatial tuning as a function of stimulus intensity of single neurons in awake macaque monkey auditory cortex. Soc Neurosci Abstr 27:512.517.
Xiao J, Huang X (2015) Distributed and Dynamic Neural Encoding of Multiple Motion Directions of Transparently Moving Stimuli in Cortical Area MT. J Neurosci 35:16180-16198.
Xiao J, Niu YQ, Wiesner S, Huang X (2014) Normalization of neuronal responses in cortical area MT across signal strengths and motion directions. J Neurophysiol 112:1291-1306.
Zohary E, Shadlen MN, Newsome WT (1994) Correlated neuronal discharge rate and its implications for psychophysical performance. Nature 370:140-143.